# Dalton Transactions

Accepted Manuscript

ROYAL SOCIETY OF CHEMISTRY

www.rsc.org/dalton

Journal Name

ARTICLE

# pH-Controlled Assembly of Two Novel Dawson-Sandwiched Clusters Involving *In Situ* Reorganization of Trivacant α-$[P_2W_{15}O_{56}]^{12-}$ into Divacant α-$[P_2W_{16}O_{57}]^{8-}$

Received 00th January 20xx,
Accepted 00th January 20xx

DOI: 10.1039/x0xx00000x

**www.rsc.org/CrystEngComm**

Ling-Yu Guo,[a,‡] Marko Jagodič,[b,‡] Su-Yuan Zeng,[c] Zhi Wang,[a] Zhi-Qiang Shi,[a] Xing-Po Wang,[a] Chen-Ho Tung,[a] Di Sun*,[a]

Modified classical trivacant Wells-Dawson α-$[P_2W_{15}O_{56}]^{12-}$ and the assembly of related sandwiched transition metal clusters are of interest but surprising scarce because of the mutability of α-$[P_2W_{15}O_{56}]^{12-}$ sensitive to assembly environments. Herein, we describe the pH-controlled assembly of two novel Dawson-sandwiched clusters $(H_2bpz)_6[Co_2(P_2W_{16}O_{57})_2]\cdot 22H_2O$ (**1**, bpz = 3,3',5,5'-tetramethyl-4,4'-bipyrazole) and $(H_2bpz)_6[Co_3H_2(P_2W_{16}O_{57})(P_2W_{15}O_{56})(H_2O)]\cdot 12H_2O$ (2) involving *in situ* transformation of α-$[P_2W_{15}O_{56}]^{12-}$. Both clusters have been characterized by X-ray single-crystal diffraction, FT-IR spectroscopy, UV-Visible spectroscopy, thermogravimetric analysis, powder X-ray diffraction, and elemental analyses. X-ray crystallography showed both heteropolytungstates become to divacant α-$[P_2W_{16}O_{57}]^{8-}$ and symmetrically encapsulate two edge-shared $CoO_6$ octahedra in the interior in **1**, while only one divacant α-$[P_2W_{16}O_{57}]^{8-}$ is observed in **2**, which combined with another trivacant α-$[P_2W_{15}O_{56}]^{12-}$ to asymmetrically clamp three edge-shared $CoO_6$ octahedra. The α-$[P_2W_{16}O_{57}]^{8-}$ heteropolytungstate should be *in situ* generated from the α-$[P_2W_{15}O_{56}]^{12-}$ *via* self-decomposition equilibria in solution. The electrochemistry behaviors of them show characteristic multi-electrons redox process relating to $W^{VI}$ centers. The electrocatalytic reduction performances toward nitrite, hydrogen peroxide, chlorate, bromate and iodate are fully measured and discussed. Especially, both of them exhibit better electrocatalytic activities toward to the reduction of bromate. Magnetic measurements indicate weak ferromagnetic exchange interactions between Co atoms sandwiched by vacant polyoxometalates.

## Introduction

Polyoxometalates (POMs) have find an important niche in the area of inorganic chemistry and material science owing to their rich structural motif and potential applications in many fields such as catalysis, nanotechnology, sensor, magnetism, and medicine delivery.[1] Although Keggin-, Wells-Dawson-, Waugh-, Lindquist-, Silverton- and Anderson-type POMs have been advanced largely,[2] modification of these classical cluster structure to form much more novel POM species or related inorganic-organic hybrids is still a hot but challenge project. There are many ways to realize above targets, such as partial reduction of $W^{VI}$ or $Mo^{VI}$ to their V/VI mixed valent counterparts, called heteropolyblue,[3] replacement of heteroatom within the cluster,[4] knockout of surface $MO_6$ (M = W or Mo) polyhedra to form diverse vacant POMs,[5] usage of the surface terminal O atoms to extend transition-metal or rare-earth ions and organic ligand to the POM-based inorganic-organic network,[6] and vacant POMs sandwiched transition-metal clusters.[7] Among such rich decoration strategies, the last is especially fascinating due to the novelties from the facile variability of vacant POM as well as the assembly challenge from polynuclear metal-oxo aggregates.

In vacant POMs family, mono- to trivacant species of the Keggin ($[XM_{12}O_{40}]^{n-}$) and the Dawson ($[X_2M_{18}O_{62}]^{n-}$, where X = $Si^{IV}$, $Ge^{IV}$, $P^{V}$, and $S^{VI}$; M = $W^{VI,V}$ $Mo^{VI,V}$) clusters have long been recognized as nucleophilic ligands for gathering transition-metal or rare-earth ions at the high-active vacant sites.[8] Recently, trivacant α-$[P_2W_{15}O_{56}]^{12-}$ was found to be an instable inorganic building unit that can experience facile reorganization to form its mono- or divacant derivatives, α-$[P_2W_{17}O_{61}]^{10-}$ and α-$[P_2W_{16}O_{59}]^{12-}$, respectively, which is due to self-decomposition equilibria existed in solution.[9] In addition to the skeletal change of cluster, the protonation states also sensitively followed the solution pH.[10] The above two behaviours of trivacant α-$[P_2W_{15}O_{56}]^{12-}$ dictate the formation of two novel sandwich POMs in this work.

Since the first synthesis of the trivacant α-$[P_2W_{15}O_{56}]^{12-}$ sandwiched compounds ($[M_4(P_2W_{15}O_{56})_2(H_2O)_2]^{16-}$, M = Co, Cu, Zn) by Finke and Droege thirty years ago,[11] many novel sandwich POMs based on trivacant α-$[P_2W_{15}O_{56}]^{12-}$ with 2-7 metal centers encapsulated have been isolated and related magnetic properties and catalytic performances were evaluated.[12] However, the sandwich POMs based on the variants of α-$[P_2W_{15}O_{56}]^{12-}$ are very rare, although what we have known is the instability of α-$[P_2W_{15}O_{56}]^{12-}$ in high temperature reaction systems. In 2008, Kögerler group isolated a semi-sandwich POM by reaction of trivacant α-$[P_2W_{15}O_{56}]^{12-}$ and bowl-shaped $[Ce^{IV}Mn^{IV}_6O_9(O_2CCH_3)_9(NO_3)(H_2O)_2]$ cluster at 70 °C. Interestingly, the trivacant α-$[P_2W_{15}O_{56}]^{12-}$ was changed to divacant α-$[P_2W_{16}O_{57}(OH)_2]^{10-}$ during assembly.[13] Following their work, Cronin

---

[a] *Key Lab of Colloid and Interface Chemistry, Ministry of Education, School of Chemistry and Chemical Engineering, Shandong University, Jinan, 250100, P. R. China. Email: dsun@sdu.edu.cn*
[b] *Faculty of Civil and Geodetic Engineering & Institute of Mathematics, Physics and Mechanics, University of Ljubljana, Jamova 2, 1000 Ljubljana, Slovenia.*
[c] *School of Chemistry and Chemical Engineering, Liaocheng University, Liaocheng, People's Republic of China.*
[‡] *These authors contributed equally.*

† Electronic Supplementary Information (ESI) available. Detailed synthesis procedure, tables, crystal data in CIF files, IR, TGA and powder X-ray diffractogram for **1** and **2**. CCDC 1449923-1449924. For ESI and crystallographic data in CIF or other electronic format see DOI: 10.1039/b000000x.

group synthesized a novel Dawson-based trimeric $[K@(Co_2P_2W_{16}O_{60})_3]^{23-}$ cluster, in which divacant $\{P_2W_{16}\}$ species is *in situ* generated by removal of two adjacent $WO_6$ octahedra from the "belt" region of non-vacant $K_6[\alpha\text{-}P_2W_{18}O_{62}]$.[14] Thus, the formation of divacant $\{P_2W_{16}\}$ species in known examples are usually sporadic and the more difficult is incorporating it into novel sandwich POMs, and both that we have eagerly pursued.

**Scheme 1.** The polyhdedra representation of classical trivacant $\alpha\text{-}[P_2W_{15}O_{56}]^{12-}$ (left) and rare bivacant $\alpha\text{-}[P_2W_{16}O_{57}]^{8-}$ (right) POMs.

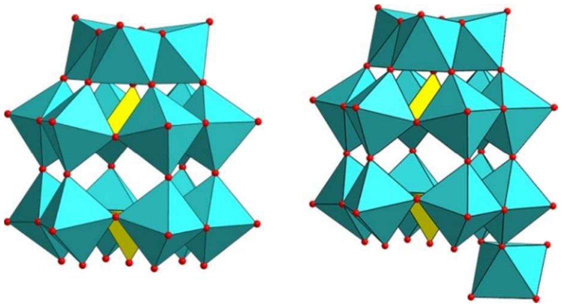

We herein present two novel $Co^{II}$ sandwich POMs based on *in situ* generated $\alpha\text{-}[P_2W_{16}O_{57}]^{8-}$ from classical trivacant $\alpha\text{-}[P_2W_{15}O_{56}]^{12-}$ (Scheme 1). At different pH value (Scheme 2), trivacant $\alpha\text{-}[P_2W_{15}O_{56}]^{12-}$ completely or partially transformed to $\alpha\text{-}[P_2W_{16}O_{57}]^{8-}$ POM, then encapsulated different $Co_n^{II}$-oxo clusters (n = 2 or 3) to form $(H_2bpz)_6[Co_2(P_2W_{16}O_{57})_2]\cdot 8H_2O$ (**1**, bpz = 3,3',5,5'-tetramethyl-4,4'-bipyrazole) and $(H_2bpz)_6[Co_3H_2(P_2W_{16}O_{57})(P_2W_{15}O_{56})(H_2O)]\cdot 12H_2O$ (**2**). This work provides a new pH-control strategy route to construction of rare $\alpha\text{-}[P_2W_{16}O_{57}]^{8-}$ POM-based sandwich clusters with adjustable $Co^{II}$/POM ratio.

**Scheme 2.** The schematic representation of assembly details of **1** and **2**

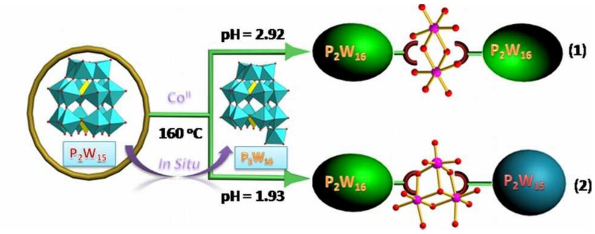

## Experimental

**Methods.** Commercially available solvents and metal salts were used without further purification. The trivacant $Na_{12}[\alpha\text{-}P_2W_{15}O_{56}]\cdot 18H_2O$ was prepared according to the literature.[15] IR spectra were recorded on a PerkinElmer Spectrum Two in the frequency range of 4000-400 $cm^{-1}$. Elemental analyses for C, H, and N were performed on a PerkinElmer 2400 CHN elemental analyzer and, for P, W, and Co, were determined with a PLASMASPEC (I) ICP atomic emission spectrometer. Powder X-ray diffraction (PXRD) data were collected on a Philips X'Pert Pro MPD X-ray diffractometer with Mo $K_\alpha$ radiation equipped with an X'Celerator detector. Thermogravimetric analyses (TGA) were performed on a SHIMADZU DTG-60A thermal analyzer from room temperature to 800 ° C under nitrogen atmosphere at a heating rate of 10° C/min. The diffuse-reflectance spectrum were performed on UV-Vis spectrophotometer (Evolution 220, ISA-220 accessory, Thermo Scientific) using a built-in 10 mm silicon photodiode with a 60 mm Spectralon sphere. The variable-temperature magnetic susceptibilities were collected on a Magnetic Property Measurement System (MPMS), SQUID-VSM (superconducting quantum interference device-vibrating sample magnetometer) (Quantum Design, USA). The electrochemical measurements were carried out on a CHI 660E electrochemical workstation (CH Instruments, Shanghai Chenghua Co.) with a conventional three-electrode cell consisting of a Pt plate as the counter electrode. The Ag/AgCl (3 M KCl filled) was used as the reference electrode. The working electrode was prepared as following: 100 mg graphite powder and 30 mg sample **1** or **2** were mixed, and ground together by a gate mortar and pestle to achieve an even, dry mixture; to the mixture 300 L paraffin oil was added under stirring with a glass rod; then the mixture was packed into 3 mm inner diameter glass tube, and the surface was pressed tightly onto weighing paper with a copper rod through the back. Electrical contact was established with copper rod through the back of the electrode. Prior to measurement, the electrolyte was thoroughly bubbled by purging it with nitrogen.

**Synthesis of 1 and 2**

A mixture of $Na_{12}[P_2W_{15}O_{56}]\cdot 24H_2O$ (44.3 mg, 0.01 mmol), $Co(NO_3)_2\cdot 6H_2O$ (58.2 mg, 0.2 mmol), and 3,3',5,5'-tetramethyl-4,4'-bipyrazole (9.5 mg, 0.05 mmol) is dissolved in 6 mL $H_2O$, then the pH was adjusted to 2.05 by addition of 1 M HCl, and stirred for 5 min at room temperature. The resulting mixture was sealed in a 25 mL Teflon-lined stainless steel autoclave and heated at 160 °C for 3000 min, after which, it was cooled over 13 h to room temperature. The product was obtained as brown rod crystals (Yield: 51.2% based on W). Elemental analysis: Anal. Calcd (%) for $C_{60}H_{112}N_{24}Co_2P_4W_{32}O_{122}$: C, 7.79; N, 3.64; H, 1.22; P, 1.34; Co, 1.27; W, 63.62 found: C, 7.67; N, 3.65; H, 1.25; P, 1.43; Co, 1.23; W, 63.73. Selected IR peak ($cm^{-1}$): 3671 (w), 2988 (w), 2903 (w), 1583 (w), 1524 (w), 1405 (w), 1260 (w), 1087 (m), 943 (m), 745 (s), 585 (s), 523 (s)

The synthesis of **2** was similar to that of **1**, but the pH was adjusted to 1.84 by addition of 1 M HCl. The red brown plate crystals was obtained (Yield: 49.8 % based on W). Elemental analysis: Anal. Calcd (%) for $C_{60}H_{124}N_{24}Co_3P_4W_{31}O_{126}$: C, 7.84; N, 3.65; H, 1.36; P, 1.35; Co, 1.92; W, 61.96. found: C, 7.78; N, 3.60; H, 1.42; P, 1.42; Co, 1.86; W, 61.79. Selected IR peak ($cm^{-1}$): 3502 (w), 1591 (w), 1527 (w), 1423 (w), 1267 (w), 1084 (m), 950 (m), 884 (m), 744 (s), 583 (s), 511 (s)

**Table 1.** Crystal data for **1** and **2**.

| Compound | **1** | **2** |
|---|---|---|
| Empirical formula | $C_{60}H_{96}Co_2N_{24}O_{122}P_4W_{32}$ | $C_{60}H_{96}Co_3N_{24}O_{126}P_4W_{31}$ |
| Formula weight | 9230.54 | 9169.62 |
| Temperature/K | 298.15 | 298.15 |
| Crystal system | triclinic | monoclinic |
| Space group | P-1 | $P2_1/c$ |
| a/Å | 15.082(2) | 24.592(3) |
| b/Å | 15.392(2) | 14.2596(17) |
| c/Å | 20.427(3) | 24.846(3) |
| α/° | 78.8374(13) | 90.00 |
| β/° | 82.5853(13) | 111.4003(10) |
| γ/° | 75.4572(12) | 90.00 |
| Volume/Å$^3$ | 4487.0(11) | 8112.0(17) |
| Z | 1 | 2 |
| $\rho_{calc}$g/cm$^3$ | 3.416 | 3.754 |

| | | |
|---|---|---|
| $\mu$/mm$^{-1}$ | 20.727 | 22.327 |
| F(000) | 4082.0 | 8134.0 |
| Reflections collected | 78602 | 45258 |
| Independent reflections | 17648 | 15970 |
| $R_{int}$ | 0.0565 | 0.0581 |
| Data/parameters | 17648/1096 | 15970/1136 |
| GOF | 1.078 | 1.020 |
| Final R indexes [I>=2σ (I)] | $R_1$ = 0.0399<br>$wR_2$ = 0.1006 | $R_1$ = 0.0411<br>$wR_2$ = 0.0848 |
| Final R indexes [all data] | $R_1$ = 0.0610<br>$wR_2$ = 0.1084 | $R_1$ = 0.0760<br>$wR_2$ = 0.0987 |

## Results and discussion

### Synthetic Aspects and General Characterizations

According to incomplete statistics, in 50 reported [$P_2W_{15}$]-based sandwich clusters, we found only one compound[12j] were synthesized in hydrothermal condition and others were isolated using stirring method at temperature no higher than 100 °C, then growth of single crystals at room temperature. These facts suggested the possible transformation or decomposition of α-[$P_2W_{15}O_{56}$]$^{12-}$ at higher temperature. Thus, we adopted this less dominant method to assemble novel sandwich clusters from common α-[$P_2W_{15}O_{56}$]$^{12-}$. On the other hand, targeted sandwich POMs synthesis can be realized by elaborate adjustment of the assembly environments such as stoichiometric ratio of reactant, solvent, pH, counterions, and temperature.[16] In this system, low pH favors the formation of them and the lower pH environment is essential to formation of **2**, but neither of them can be alternatively isolated by changing Co/α-[$P_2W_{15}O_{56}$]$^{12-}$ stoichiometry, despite this is different in the final structures of **1** and **2**. The achievement of different pH is controlled by adding the different amount of 1 M HCl solution. The detail yield-pH correlations for **1** and **2** are plotted in Figure 1. The best pH values for synthesis of them are 2.05 and 1.84, respectively. The different reaction temperatures (120, 140, 160 and 180 °C) were also tried in the synthesis of **1** and **2**. The best yields are obtained at 160 °C for them. Only **2** could be isolated at 140 °C with a lower yield of 28 %. Whereas only brown precipitates were found after reaction at 180 or 120 °C for **1** and **2**. Both of them can be readily prepared in high purity with *ca.* 50% isolated yield under the optimal reaction conditions.

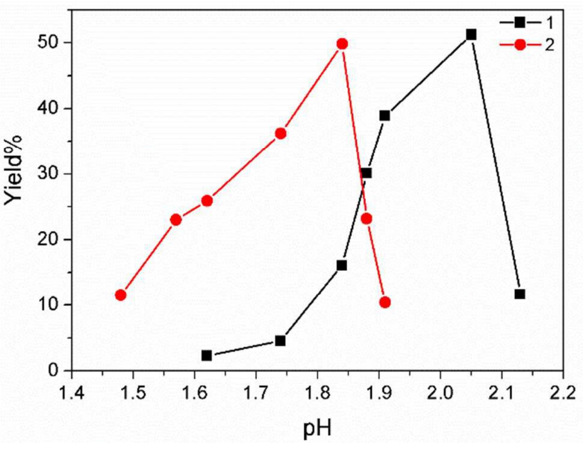

**Figure 1.** The plot of reaction pH value vs yield for synthesis of **1** and **2**.

Compared PXRD patterns (Figure S1) indicate both **1** and **2** are pure phases for the following characterizations. In IR spectra (Figure S2), P-O stretching peaks appeared at 1087 and 1085 cm$^{-1}$, for **1** and **2** respectively.[17] The classical W-O and W-O-W bands are shown in the region lower than 1000 cm$^{-1}$.[18a] The TGA curves (Figure S3) of them show similar two steps weight losing behaviour and the first weight loss of 4.1% (calc. 4.2%) and 2.9% (calc. 2.5%) for **1** and **2** occur at 123 and 127 °C, respectively. The strong adsorption band below 300 nm should be attributed to $O_{2p}\rightarrow W_{5d}$ charge transfer transitions[18b] and the *d*-*d* absorption bands contributed by Co$^{II}$ ions were observed as a weak shoulder peaks at around 580 nm for **1** and **2**, as indicated in the solid-state diffusion-reflection UV-Vis spectra (Figure S4).

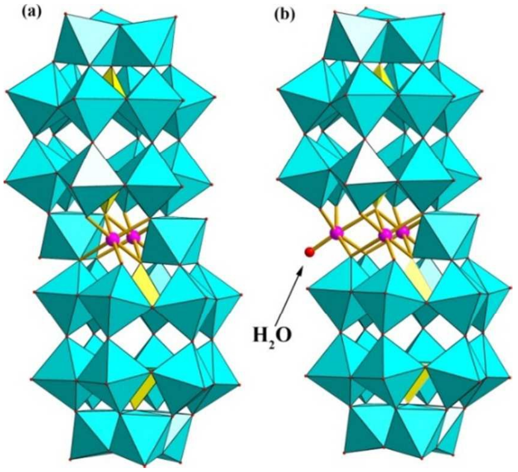

**Fig 2.** Side view of structures of the polyanion **1** (a) and **2** (b). All $PO_4$ units highlighted as yellow tetrahedra and all $WO_6$ units in cyan octahedra. The sandwiched Co ions were shown as purple balls.

### Cluster Structures of 1 and 2

X-ray diffraction on claret-red single crystals of **1** and **2** show they crystallize in the triclinic *P*-1 and monoclinic *P*2$_1$/c space groups, respectively (Table 1). Both asymmetric units of **1** and **2** contain a half of complete cluster imposed by crystallographic inversion center. The bond valence sum calculations indicate that all Co and W centers are +2 and +6 oxidation state, respectively (Table S1). In **1**, the reactant trivacant α-[$P_2W_{15}O_{56}$]$^{12-}$ has *in situ* gained an extra tungsten site of W16 atom, and thus is transformed to a rare divacant derivative of Dawson {$P_2W_{18}$}, which further binds two edge-shared but not corner-linked CoO6 octahedra (Co-O =1.993(9) - 2.191(8) Å; Co···Co = 3.24 Å) in the interior using the O atoms at the lacuna position to form the resulting sandwich cluster with an overall $C_i$ symmetry (Figure 2a). Alternatively, the anionic cluster of **1** also could be described to a layer of two internal Co ions and two external W ions, which is sandwiched by two trivacant α-[$P_2W_{15}O_{56}$]$^{12-}$ units upper and lower.

Interestingly, for **2**, two slices of "bread" are different to that in **1**, one trivacant α-[$P_2W_{15}O_{56}$]$^{12-}$ and another bivacant α-[$P_2W_{16}O_{57}$]$^{8-}$ (Figure 2b), and the "meat" layer is also dissimilar to that in **1**. Three CoO6 octahedra (Co-O = 1.993(9) - 2.178(9) Å; Co···Co = 3.19 - 3.33 Å) are edge-shared to form a defected cube, then asymmetrically clamped by one trivacant α-[$P_2W_{15}O_{56}$]$^{12-}$ and one bivacant α-[$P_2W_{16}O_{57}$]$^{8-}$. Since the external Co1 and W1 statistically occupied, molecular symmetry of **2** is essentially an overall $C_s$ point group, although the sandwich anion of **2** sits on an inversion center in the crystallography. Until now, there are only two bivacant α-

$[P_2W_{16}O_{57}]^{8-}$ based compounds.[13,14] One is *in situ* transformed from trivacant α-$[P_2W_{15}O_{56}]^{12-}$, giving a half-sandwich cluster, whereas another is a trimer of $[Co_2P_2W_{16}O_{60}]^{8-}$ from non-vacant [α-$P_2W_{18}O_{62}]^{6-}$. However, the genuine sandwich POM cluster from *in situ* generated bivacant α-$[P_2W_{16}O_{57}]^{8-}$ is unprecedented.

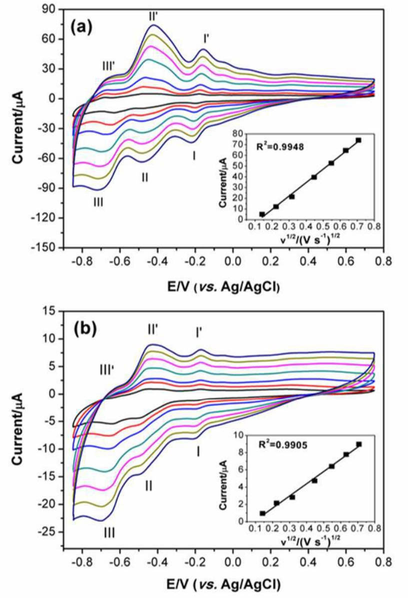

**Figure 3.** Cyclic voltammograms of (a) **1**-GCE, (b) **2**-GCE in 0.5 M $Na_2SO_4$-$H_2SO_4$ aqueous solutions (pH = 2.52) at different scans (from inner to outer: 20, 50, 100, 200, 300, 400, 500 mV $s^{-1}$ ). Inset: variation of the second cathodic peak current intensity as a function of the square root of the scan rate.

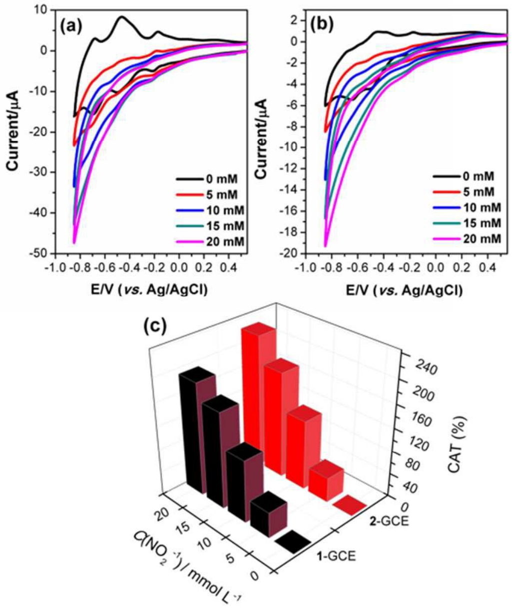

**Figure 4.** Cyclic voltammograms showing the electrocatalytic activity of (a) **1**-GCE, (b) **2**-GCE in 0.5 M $Na_2SO_4$-$H_2SO_4$ aqueous solutions (pH = 2.52) with scan rate of 20 mV $s^{-1}$, in the presence of different concentration of nitrite. (c) Graph of CAT versus concentration of $NO_2^-$ for **1**-GCE and **2**-GCE, (*I*p values of cathodic peak at -0.85 V for $NO_2^-$).

### Electrochemical properties and electrocatalytic activities of 1 and 2.

The Naphthol-modified glassy carbon electrode (GCE) were fabricated as working electrode to investigate the electrochemical properties of **1** and **2** in 0.5 M $Na_2SO_4$-$H_2SO_4$ aqueous solutions (pH = 2.52) using cyclic voltammograms (CV). As shown in Figure 3, the potentials of three pairs of reversible redox peaks are -0.180 and -0.201 V (I–I'), -0.454 and -0.489 V (II–II'), -0.633 and -0.679 V (III–III') for **1**-GCE and -0.172 and -0.212 V (I–I'), -0.442 and -0.518 V (II–II'), -0.644 and -0.70 V (III–III') for **2**-GCE, respectively. The half-wave potentials $E_{1/2}$ = ($E$pa + $E$pc)/2 of I/I', II/II', and III/III' are -0.190, -0.470 and -0.656 V for **1**-GCE, and -0.192, -0.480 and -0.672 V for **2**-GCE (scan rate: 20 mV $s^{-1}$), which are ascribed to the multi-electrons redox process of $W^{VI}$ centers,[19] whereas redox peaks of $Co^{II}$ ions were not observed under our experimental conditions. Moreover, the peak current of the second cathodic wave is proportional to the square root of the scan rate between -0.85 to 0.75 V, suggesting a diffusion-controlled redox process (see inset plots in Figure 3a and 3b).

The electrocatalytic reduction activities toward nitrite, hydrogen peroxide, chlorate, bromate, iodate are fully studied in 0.5 M $Na_2SO_4$-$H_2SO_4$ aqueous solutions (pH = 2.52) using CVs with the scan rate of 20 mV $s^{-1}$. The catalytic efficiency is defined as CAT = [$I_p$ (POM, substrate) – $I_p$ (POM)] / $I_p$ (POM) × 100%, where $I_p$(POM, substrate) and $I_p$(POM) are the peak currents for the reduction of the POM with and without the presence of substrate (nitrite, hydrogen peroxide and so on).[20] Figure 4a and 4b showed that **1**- and **2**-GCE have moderate electrocatalytic activity towards the reduction of nitrite, as revealed by the changes peak current upon the addition of nitrite, that is, the cathodic current gradually increases with a continuous increase in the concentration of nitrite, while the corresponding anodic current decreases. Based on the reduction peak currents at -0.85 V, the catalytic efficiencies (CAT) of **1**-GCE are calculated to 0%, 43.6%, 106.7%, 165%, 193%, corresponding to the concentration of nitrite varied from 0 to 20 mM, whereas the CAT values for **2**-GCE are 0%, 42.2%, 120.37%, 182.6%, 226.5% under the same measurement condition, which indicates that **2**-GCE is better than **1**-GCE on electrocatalytic reduction of nitrite (Figure 4c).

As shown in Figure S5a and S5b, the **1**- and **2**-GCE also exhibit electrocatalytic reduction ability to $H_2O_2$ in the potential range of -0.85 - 0.75 V. For **1**-GCE, with the addition of $H_2O_2$, the reduction peak (III) currents increase while the corresponding oxidation peak currents decrease. Additionally, the second redox peaks gradually become undistinguished and the first redox peak currents are almost constant with the increase concentration of $H_2O_2$, which indicates they has negligible electrocatalytic contributions to the reduction of $H_2O_2$. For **2**-GCE, the redox peak profiles dramatically changed along with the increase of the concentration of $H_2O_2$, but the gradually increased cationic peak currents are still observed in -1 - 0V, suggesting its electrocatalytic activity towards to the reduction of $H_2O_2$. The highest CAT values are 334.0% and 242.0% for **1**- and **2**-GCE, respectively, when the concentration of $H_2O_2$ is 60 mM.

The electrocatalytic reduction abilities of **1**- and **2**-GCE toward $ClO_3^-$, $BrO_3^-$ and $IO_3^-$ are evaluated in the same electrolyte using cyclic voltammograms (CV). As shown in Figure S6a-S6h, it was clearly seen that both **1**- and **2**-GCE should have the same order of electrocatalytic reduction abilities toward $XO_3^-$ (X= Cl, Br and I), that is, $BrO_3^-$, $IO_3^-$, and $ClO_3^-$. As given in Figure S6b and S6e, for both **1**- and **2**-GCE, the second (II) and the third (III) reduction peak currents increase while the corresponding oxidation peak currents decrease when increasing concentration of $BrO_3^-$. The increment of the third reduction peak currents are much larger than the second one, suggesting that the third reduction peak mainly contributes the electrocatalytic activity to the $BrO_3^-$ reduction. In addition, the first redox peaks are nearly constant upon addition of $BrO_3^-$, indicating the little electrocatalytic contribution to the $BrO_3^-$ reduction. Differently, with the addition of $IO_3^-$, all reduction peak currents increase with similar degrees while the corresponding oxidation peak currents decrease, which indicates that all reduction peaks have electrocatalytic activity to $IO_3^-$ reduction. The best electrocatalytic reduction performances of **1**- and **2**-GCE on $BrO_3^-$ are further proved by counting the CAT values of them as shown in Figure S6g and S6h. For example, the CAT values of **1**-GCE are 8.6%, 231.67%, 62.7%, respectively, when the concentration of $ClO_3^-$, $BrO_3^-$, $IO_3^-$ reaches to 6 mM. The electrocatalytic reduction efficiency to $BrO_3^-$ is 27 times higher than that to $ClO_3^-$, and 3.7 times higher than that to $IO_3^-$, which indicates the selectively electrocatalytic ability toward low concentration of $BrO_3^-$ with **1**-GCE. A similar electrocatalytic reduction performances are also found for **2**-GCE. These results are well accordant with the strongest oxidization ability of $BrO_3^-$ with respect to the others.[21] Furthermore, the electrocatalytic efficiencies of **1**- and **2**-GCE are also compared in Figure S6g-S6h, **1**-GCE has higher CAT value than **2**-GCE towards the reduction of $ClO_3^-$, $BrO_3^-$ and $IO_3^-$. In the electrolyte solution containing 4 mM $ClO_3^-$, $BrO_3^-$, $IO_3^-$, the corresponding CAT values of **1**-GCE are 5.7%, 160.0%, 39.8%, and those of **2**-GCE are only 2.0%, 60.2%, 23.3%.

**Magnetic properties**

The temperature dependence of the magnetic susceptibility $\chi(T)$ of **1** and **2** was investigated between 2 K and 300 K in a magnetic field of 1000 Oe. Magnetization curves $M(H)$ where measured at 2 K in magnetic fields up to 80 kOe. All magnetic measurements were performed on a SQUID magnetometer. Before analysis the data were corrected for sample holder contribution and the Larmor core diamagnetic contribution as obtained from Pascal's tables.[22]

The $\chi T(T)$ curves for both samples (inset on Figure 5) are constant above approximately 50 K and increase when approaching lower temperatures, which indicates ferromagnetic interactions between Co centers. By fitting the $\chi(T)$ data (Figure 5) with the Curie-Weiss model, $\chi = C/(T-\theta)$, above 50 K a Curie constant $C = 10.5\,\mathrm{emu\,K/mol}$ and a Curie-Weiss temperature $\theta = 7.2\,\mathrm{K}$ were obtained for 1, yielding an effective magnetic moment $\mu_{eff} = \sqrt{8\chi T} = 6.5\,\mu_B$ per Co atom. This value matches $6.54\,\mu_B$ which is the theoretical value for Co(II) atoms when $J = |L+S|$.[23] For 2 $C = 6.9\,\mathrm{emu\,K/mol}$ and $\theta = 4.1\,\mathrm{K}$ were obtained, yielding an effective magnetic moment $\mu_{eff} = 4.3\,\mu_B$ per Co atom, which is closer to $4.8\,\mu_B$ the usually measured value for Co(II) ions with non-zero orbital contribution to the magnetic moment.[24] Positive values of $\theta$ for both samples further support weak ferromagnetic interactions between Co atoms.

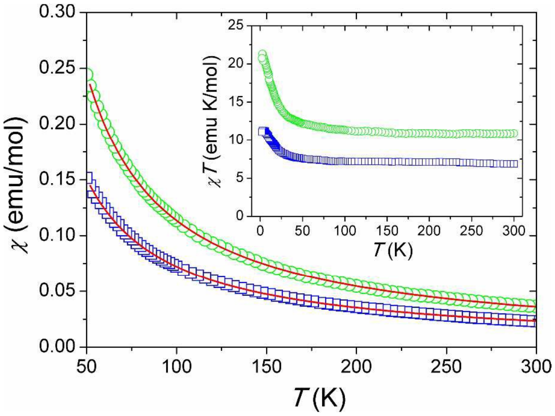

**Figure 5.** Temperature dependence of magnetic susceptibility measured at 1000 Oe for samples **1** (green circles) and **2** (blue squares). The corresponding Curie-Weiss fits are shown as red full lines. In the inset the $\chi T(T)$ curves are shown.

The magnetic field dependences of magnetization for **1** and **2** are shown in Figure 6. The curves do not show any coercivity and both saturate above 20 kOe. The data were fitted with the function

$$M = M_0 B_J\left(\frac{gJ\mu_B H}{k_B T}\right),$$

where $M_0$ is the saturation magnetization, $B_J$ is the Brillouin function, $g$ the g-factor, $J$ the total angular momentum and $\mu_B$ the Bohr magneton. For **1** the values $g$ = 4.8 and $J$ = 2.8 were obtained, whereas for **2** $g$ = 4.4 and $J$ = 2.2 gave the best fit. Both values for $g$ are close to 4.3 which is the approximate value for a Co(II) atom with octahedral coordination.[22] The obtained $J$ values for both samples are close to 5/2, which is the theoretical value for a Co(II) atom.

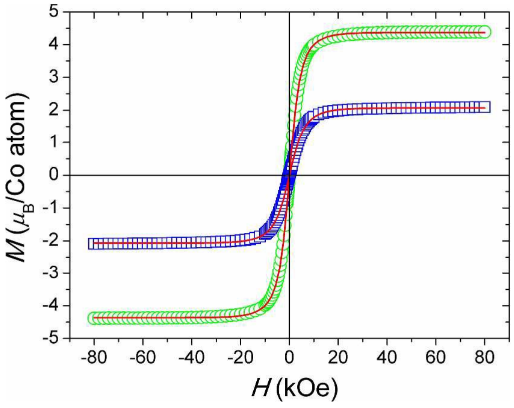

**Figure 6.** Magnetization curves versus magnetic field measured at 2 K for samples **1** (green circles) and **2** (blue squares). The fits with the Brillouin function are shown as red full lines.

## Conclusions

We isolated and structurally characterized two novel Dawson-sandwiched clusters, the formation of which are depended on pH values and involves completely or partially *in situ* transformation of trivacant α-$[P_2W_{15}O_{56}]^{12-}$ to rare divacant α-$[P_2W_{16}O_{57}]^{8-}$. The sandwiched $Co_n^{II}$-oxo clusters are also different in 1 and 2, thus giving an adjustable $Co^{II}$/POM ratio. Characteristic multi-electrons redox process relating to $W^{VI}$ centers are also found in cyclic voltammograms. Both of them exhibit best electrocatalytic activities toward to the reduction of bromate, compared to chlorate and iodate. Intra-cluster weak ferromagnetic interactions between $Co^{II}$ atoms of both 1 and 2 are confirmed by magnetic susceptibility measurements. This work demonstrated here releases a new approach to controllable strategy for assembly and functionalization of POM-based materials for various applications.

## Acknowledgements

This work was supported by the NSFC (Grant Nos. 21201110 and 21571115), Young Scholars Program of Shandong University (2015WLJH24), and The Fundamental Research Funds of Shandong University (104.205.2.5 and 2015JC045). Marko Jagodič is funded by Slovenian Research Agency (ARRS), Program Number P2-0348.

## Notes and references

1. (a) M. T. Pope and A. Muller, *Angew. Chem., Int. Ed., Eng.* 1991, ***30***, 34; (b) E. Coronado and C. J. Gomez-Garcia, *Chem Rev* 1998, ***98***, 273; (c) A. Dolbecq, E. Dumas, C. R. Mayer and P. Mialane, *Chem Rev* 2010, ***110***, 6009; (d) J. T. Rhule, C. L. Hill and D. A. Judd, *Chem Rev* 1998, ***98***, 327; (e) M. Sadakane and E. Steckhan, *Chem Rev* 1998, ***98***, 219-237. E. Cadot, M. N. Sokolov, V. P. Fedin, C. Simonnet-Jegat, S. Floquet and F. Secheresse, *Chemical Society Reviews* 2012, ***41***, 7335; (f) D.-Y. Du, J.-S. Qin, S.-L. Li, Z.-M. Su and Y.-Q. Lan, *Chem. Soc. Rev.*, 2014, ***43***, 4615; (g) H. Lv, Y. V. Geletii, C. Zhao, J. W. Vickers, G. Zhu, Z. Luo, J. Song, T. Lian, D. G. Musaev and C. L. Hill, *Chem. Soc. Rev.*, 2012, ***41***, 7572; (h) H. N. Miras, L. Vila-Nadal and L. Cronin, *Chem. Soc. Rev.*, 2014, ***43***, 5679; (i) S.-S. Wang and G.-Y. Yang, *Chem Rev* 2015, ***115***, 4893; (j) Y.-F. Song and R. Tsunashima, *Chem. Soc. Rev.*, 2012, ***41***, 7384; (k) Y. Wang and I. A. Weinstock, *Chem. Soc. Rev.*, 2012, ***41***, 7479; (l) T. Hirano, K. Uehara, K. Kamata and N. Mizuno, *J Am Chem Soc* 2012, ***134***, 6425; (m) K. Kamata, K. Yonehara, Y. Nakagawa, K. Uehara and N. Mizuno, *Nat Chem* 2010, ***2***, 478;
2. (a) J. M. Clemente-Juan and E. Coronado, *Coord. Chem. Rev.*, 1999, ***193-5***, 361; (b) D.-Y. Du, L.-K. Yan, Z.-M. Su, S.-L. Li, Y.-Q. Lan and E.-B. Wang, *Coord. Chem. Rev.*, 2013, ***257***, 702; (c) W.-W. He, S.-L. Li, H.-Y. Zang, G.-S. Yang, S.-R. Zhang, Z.-M. Su and Y.-Q. Lan, *Coord. Chem. Rev.*, 2014, ***279***, 141; (d) C. Yvon, A. Macdonell, S. Buchwald, A. J. Surman, N. Follet, J. Alex, D. L. Long and L. Cronin, *Chem Sci* 2013, ***4***, 3810; (e) P. F. Wu, P. C. Yin, J. Zhang, J. Hao, Z. C. Xiao and Y. G. Wei, *Chem-Eur J* 2011, ***17***, 12002; (f) J. Zhang, W. Li, C. Wu, B. Li, J. Zhang and L. X. Wu, *Chem-Eur J* 2013, ***19***, 8129; (g) X. L. Wang, Y. Q. Guo, Y. G. Li, E. B. Wang, C. W. Hu and N. H. Hu, *Inorg Chem* 2003, ***42***, 4135; (h) Y. Gong, T. Wu, P. G. Jiang, J. H. Lin and Y. X. Yang, *Inorg Chem* 2013, ***52***, 777; (i) Y. X. Kuang and I. R. Evans, *Inorg Chem* 2010, ***49***, 6005; (j) Y. Jia, J. Zhang, Z.-M. Zhang, Q.-Y. Li and E.-B. Wang, *Inorg Chem Commun* 2014, ***43***, 5; (k) H. Tan, W. Chen, Y.-G. Li, D. Liu, L. Chen and E. Wang, *J Solid State Chem* 2009, ***182***, 465.
3. (a) K. Yu, B. Wan, Y. Yu, L. Wang, Z. H. Su, C. M. Wang, C. X. Wang and B. B. Zhou, *Inorg Chem* 2013, ***52***, 485; (b) K. Yu, B. B. Zhou, Y. Yu, Z. H. Su and G. Y. Yang, *Inorg Chem* 2011, ***50***, 1862-1867; (c) J. Gao, J. Yan, S. Beeg, D. L. Long and L. Cronin, *J Am Chem Soc* 2013, ***135***, 1796; (d) H. Imai, T. Akutagawa, F. Kudo, M. Ito, K. Toyoda, S. Noro, L. Cronin and T. Nakamura, *J Am Chem Soc* 2009, ***131***, 13578; (e) H. N. Miras, C. J. Richmond, D. L. Long and L. Cronin, *J Am Chem Soc* 2012, ***134***, 3816; (f) H. N. Miras, M. Sorus, J. Hawkett, D. O. Sells, E. J. L. McInnes and L. Cronin, *J Am Chem Soc* 2012, ***134***, 6980.
4. (a) J. Yan, D. L. Long and L. Cronin, *Angew Chem Int Ed* 2010, ***49***, 4117; (b) M. N. Corella-Ochoa, H. N. Miras, A. Kidd, D. L. Long and L. Cronin, *Chem Commun* 2011, ***47***, 8799.
5. (a) B. Godin, Y. G. Chen, J. Vaissermann, L. Ruhlmann, M. Verdaguer and P. Gouzerh, *Angew Chem Int Ed* 2005, ***44***, 3072; (b) P. Mialane, A. Dolbecq, E. Riviere, J. Marrot and F. Secheresse, *Angew Chem Int Ed* 2004, ***43***, 2274; (c) S. G. Mitchell, P. I. Molina, S. Khanra, H. N. Miras, A. Prescimone, G. J. T. Cooper, R. S. Winter, E. K. Brechin, D.-L. Long, R. J. Cogdell and L. Cronin, *Angew Chem Int Ed* 2011, ***50***, 9154; (d) J.-W.Zhao, J. Zhang, S.-T. Zheng and G.-Y. Yang, *Chem Commun* 2008, 570; (e) S.-T. Zheng, D.-Q. Yuan, H.-P. Jia, J. Zhang, G.-Y. Yang, *Chem Commun* 2007, 1858; (f) X.-X. Li, S.-T. Zheng, J. Zhang, W.-H. Fang, G.-Y. Yang and J. M. Clemente-Juan, *Chem-Eur J* 2011, ***17***, 13032; (g) J.-W. Zhao, H.-P. Jia, J. Zhang, S.-T. Zheng and G.-Y. Yang, *Chem-Eur J* 2007, ***13***, 10030; (h) J.-W. Zhao, C.-M. Wang, J. Zhang, S.-T. Zheng and G.-Y. Yang, *Chem-Eur J* 2008, ***14***, 9223.
6. (*a*) Y. Q. Lan, S. L. Li, J. S. Qin, D. Y. Du, , X. L. Wang, Z. M. Su and Q. Fu, *Inorg Chem* 2008, ***47***, 10600; (*b*) Y. Q. Lan, S. L. Li, X. L. Wang, K. Z. Shao, D. Y. Du, H. Y. Zang and Z. M. Su, *Inorg Chem* 2008, ***47***, 8179; (c) X. L. Wang, H. L. Hu, G. C. Liu, H. Y. Lin and A. X. Tian, *Chem Commun* 2010, ***46***, 6485; (d) X. L. Wang, Y. F. Bi, B. K. Chen, H. Y. Lin and G. C. Liu, *Inorg Chem* 2008, ***47***, 2442; (e) D. B. Dang, Y. Bai, C. He, J. Wang, C. Y. Duan and J. Y. Niu, *Inorg Chem* 2010, ***49***, 1280; (f) D. B. Dang, G. S. Zheng, Y. Bai, F. Yang, H. Gao, P. T. Ma and J. Y. Niu, *Inorg Chem* 2011, ***50***, 7907; (g) X. F. Kuang, X. Y. Wu, R. M. Yu, J. P. Donahue, J. S. Huang and C. Z. Lu, *Nat Chem* 2010, ***2***, 461; (h) M.-X. Liang, C.-Z. Ruan, D. Sun, X.-J. Kong, Y.-P. Ren, L.-S. Long, R.-B. Huang and L.-S. Zheng, *Inorg Chem* 2014, ***53***, 897; (i) T.-P. Hu, Y.-Q. Zhao, Z. Jagličić, K. Yu, X.-P. Wang and D. Sun, *Inorg Chem* 2015, ***54***, 7415; (j) Y.-Q. Zhao, K. Yu, L.-W. Wang, Y. Wang, X.-P. Wang and D. Sun, *Inorg Chem* 2014, ***53***, 11046.
7. (a) S. T. Zheng and G. Y. Yang, *Chem Soc Rev* 2012, ***41***, 7623; (*b*) J.-D. Compain, P. Mialane, A. Dolbecq, I. M. Mbomekalle, J. Marrot, F. Secheresse, E. Riviere, G. Rogez and W. Wernsdorfer, *Angew Chem Int Ed* 2009, ***48***, 3077; (c) M. Ibrahim, Y. Lan, B. S. Bassil, Y. Xiang, A. Suchopar, A. K. Powell and U. Kortz, *Angew. Chem. Int. Ed.*, 2011, ***50***, 4708; (d) L. Lisnard, P. Mialane, A. Dolbecq, J. Marrot, J. M. Clemente-Juan, E. Coronado, B. Keita, P. de Oliveira, L. Nadjo and F. Secheresse, *Chem-Eur J* 2007, ***13***, 3525; (e) S. S. Mal, M. H. Dickman, U. Kortz, A. M. Todea, A. Merca, H. Boegge, T. Glaser, A. Mueller, S. Nellutla, N.Kaur, J. van Tol, N. S. Dalal, B. Keita and L. Nadjo, *Chem-Eur J* 2008, ***14***, 1186; (f) P. Mialane, C. Duboc, J. Marrot, E. Riviere, A. Dolbecq and F. Secheresse, *Chem-Eur J* 2006, ***12***, 1950; (g) B. S. Bassil, S. Nellutla, U. Kortz, A. C. Stowe, J. van Tol, N. S. Dalal, B. Keita and L. Nadjo, *Inorg Chem* 2005, ***44***, 2659; (h) L. Chen, K. Zhu, L.-H. Bi, A. Suchopar, M. Reicke, G. Mathys, H. Jaensch, U. Kortz and R. M. Richards, *Inorg Chem* 2007, ***46***, 8457; (i) Y. Hou, L. Xu, M. J. Cichon, S. Lense, K. I. Hardcastle and C. L. Hill, *Inorg Chem* 2010, ***49***, 4125; (j) B. Li, J.-W. Zhao, S.-T. Zheng and G.-Y. Yang, *Inorg Chem* 2009, ***48***, 8294; (k) H. Liu, C. Qin, Y.-G. Wei, L. Xu, G.-G. Gao, F.-Y. Li, and X.-S. Qu, *Inorg Chem* 2008, ***47***, 4166; (l) C.-M. Wang, S.-T. Zheng and G.-Y. Yang, *Inorg Chem* 2007, ***46***, 616; (m) Q.Wu, Y.-G. Li, Y.-H. Wang, E.-B. Wang, Z.-M. Zhang and R. Clerac, *Inorg Chem* 2009, ***48***, 1606.
8. (a) M. T. Pope, in *Comprehensive Coordination Chemistry II*, Elsevier, New York, 2004, vol. 4, pp. 635–678; (b) C. L. Hill, in *Comprehensive Coordination Chemistry II*, Elsevier, New York, 2004, vol. **4**, pp. 679–759; (c) D. L. Long, E. Burkholder and L. Cronin, *Chem. Soc. Rev.*, 2007**,** ***36***, 105; (d) A. Muller, F. Peters, M. T. Pope and D. Gatteschi, *Chem. Rev.*, 1998**,** ***98***, 239.
9. R. Contant and G. Herve, *Rev. Inorg. Chem.*, 2002, ***22***, 63.
10. X. Fang and C. L.Hill, *Angew. Chem., Int. Ed.*, 2007, ***46*****,** 3877.
11. R. G. Finke and M. W. Droege, *Inorg. Chem.* 1983, ***22***, 1006.
12. (a) C. P. Pradeep, D.-L. Long, P. Koegerler and L. Cronin, *Chem. Comm.*, 2007, 4254; (b) T. M. Anderson, K. I. Hardcastle, N. Okun and C. L. Hill, *Inorg. Chem.* 2001**,** ***40***, 6418; (c) L. Ruhlmann, J. Canny, R. Contant and R. Thouvenot, *Inorg. Chem.* 2002**,** ***41***, 3811; (d) J. M. Clemente-Juan, E. Coronado, A. Gaita-Arino, C. Gimenez-Saiz, H. U. Gudel, A. Sieber, R. Bircher and H. Mutka, *Inorg. Chem.* 2005**,** ***44***, 3389; (e) L. Ruhlmann, C. Costa-Coquelard, J. Canny and R. Thouvenot, *Eur. J. Inorg. Chem.*, 2007, 1493l; (f) N. H. Nsouli, M. Prinz, N. Damnik, M. Neumann, E. Talik and U. Kortz, *Eur. J. Inorg. Chem.*, 200**9**, 5096; (g) D. Schaming, J. Canny, K. Boubekeur, R. Thouvenot and L. Ruhlmann, *Eur. J. Inorg. Chem.*, 2009, 5004; (h) T. M. Anderson, X. Zhang, K. I. Hardcastle and C. L. Hill, *Inorg. Chem.* 2002**,** ***41***, 2477; (i) X. Fang, P. Koegerler, M. Speldrich, H. Schilder and M. Luban, *Chem. Comm.* 2012**,** ***48***, 1218; (j) X. Wang, S. Liu, Y. Liu, D. He, N. Li, J. Miao, Y. Ji and G. Yang, *Inorg. Chem*. 2014, ***53***, 13130.
13. X. Fang and P. Kogerler, *Chem. Comm.* 2008, 3396.
14. S. G. Mitchell, S. Khanra, H. N. Miras, T. Boyd, D.-L. Long and L. Cronin, *Chem. Comm.* 2009, 2712.
15. R. G. Finke, M. W. Droege and P. J. Domaille, *Inorg. Chem*. 1987, ***26***, 3886.
16. *Polyoxometalates*: M. T. Pope, U. Kortz in *Encyclopedia of Inorganic and Bioinorganic Chemistry*, Wiley, New York, 2012.
17. C. Rocchiccioli-Deltcheff and R. Thouvenot, *Spectrosc. Lett.* 1979, ***12***, 127.
18. (*a*) C. Rocchiccioli-Deltcheff, R. Thouvenot and R. Franck, *Spectrochim. Acta* 1976, ***22A***, 587; (*b*) E. N. Glass, J. Fielden, A. L. Kaledin, D. G. Musaev, T. Q. Lian and C. L. Hill, *Chem-Eur J* 2014, ***20***, 4297.
19. M. Sadakane and E. Steckhan, *Chem. Rev.*, 1998, ***98***, 219.
20. B. Keita, A. Belhouari, L. Nadjo and R. Contant, *J. Electroanal. Chem.*, 1995, ***381***, 243.

21. C. M. A. Brett and A. M. O. Brett, *Electrochemistry; Principles, Methods and Applications*, 1994, Oxford University Press.
22. O. Kahn, in *Molecular Magnetism*, VCH Publishers, New York, 1993.
23. N. W. Ashcroft and N. D. Mermin, *Solid State Physics*, Saunders College Publishing, USA, 1976.
24. (a) Q. Chen, M.-H. Zeng, L.-Q. Wei and M. Kurmoo, *Chem Mater* 2010, ***22***, 4328. (b) J.-Y. Zou, W. Shi, N. Xu, L.-L. Li, J.-K. Tang, H.-L. Gao, J.-Z. Cui and P. Cheng, *Chem Commun* 2013, ***49***, 8226. (c) R. Boca and R. Herchel, *Coord. Chem Rev* 2010, ***254***, 2973. (d) M. Kurmoo, *Chem Soc Rev* 2009, ***38***, 1353

# For Table of Contents Use Only

Two novel Dawson-sandwiched clusters involving *in situ* reorganization of trivacant α-[$P_2W_{15}O_{56}$]$^{12-}$ into divacant α-[$P_2W_{16}O_{57}$]$^{8-}$ were assembled under the different pH environments